NUMERICAL STUDY OF VORTEX-INDUCED VIBRATION FLEXIBLE RISER AND PIPE MODELS

Z.S. Chen,[1] W.J. Kim[*2] and J.H. Yoo[2]

해저석유 생산용 라이저 모형에 대한 Vortex-Induced Vibration 수치계산

진 정 수,[1] 김 우 전,[*2] 유 재 훈[2]

This paper summarizes the VIV-related research with the focus on flexible riser and pipe models subject to various engineering conditions. First of all, a series of numerical simulations for the purpose of validating the efficiency of FSI solution approach (ANSYS MFX) has been performed. The comparison between the simulation and the experimental data shows that the present FSI solution method is capable of giving acceptable estimation to VIV problems. As a meaningful application to engineering problems, some tentative simulation cases which are difficult to carry out in experiment, such as a flexible pipe with internal flow and multi-assembled pipes, have been successfully carried out. The coupling mechanism between vortex shedding and the VIV has been well interpreted.

Key Words : Vortex-Induced Vibration(VIV), Riser, Internal Flow, Forced Motion, Multi-Assembled Pipes, FSI

1. INTRODUCTION

Flow around a fixed or oscillating cylinder has received much attention in the past few decades. Since the current and wave propagates with high degree of complexity, the flexible risers/pipes are readily subjected to shear or oscillatory flow in real ocean conditions. As it is well known, vortex-induced vibration plays a leading role in determining the life span of marine risers. Due to the developing deep-water oil exploitation and massive use of underwater cables, the need to enhance our knowledge about vortex-induced vibration (VIV) for elastic pipe has greatly risen. A better comprehension of the vortex dynamics causing vibration and fatigue to risers is necessary.

The fact that numerical simulations of VIV have been failing to accurately duplicate experimental processes mostly attributes to the complexity of the physics involved in the real problem. It is worth noting that the separation excursion and the coupling mechanism between the vortex wake and the dynamics of the structure are the key factors. From the multi-physics point of view, fluid-structure interaction (FSI) occurs when fluid interacts with a solid structure, exerting pressure to the structure. As a result, it leads to deformation of the flexible structure, and then alters the flow conformation finally. Due to the limitation of calculation ability and some shortages of CFD software package itself, most numerical attempts are apt to 2D vortex simulations and then integrate the hydrodynamic forces to 3D fluid domain (Yamamotoa, Meneghinib et al., 2004). Some tasks to simulate vortex-induced vibration with considerably large aspect ratio are indeed a 2D numerical simulation (Holmes, Owen et al., 2006).

Grid topology and density, boundary condition, and coupling scheme between the flow governing equations and structure motion equations have strong influence on the qualities of the numerical results (Holmes, Owen,

1 목포대학교 중형조선 RIC
2 정회원, 목포대학교 해양시스템공학과
* TEL : 061) 450-2766
* Corresponding author, E-mail: kimwujoan@mokpo.ac.kr

2006). With risers presenting comparatively high aspect ratio and complex flow field around them, a complete three-dimensional simulation close to realistic conditions should be looked for. Aiming at an acceptable hydro-elastic response of the riser structure, a more robust numerical strategy should be introduced. Rapid development of commercial CFD software provides us some new choices for FSI numerical simulation. Menter has successfully simulated two kinds of FSI cases using ANSYS multi-physics software (Menter and Sharkey, 2006). It preliminarily verified the capability of MFX solver to deal with coupling fluid-structure problem.

By means of ANSYS MFX solution approach and 3D large eddy simulation model, the FSI problems related to several engineering condition have been solved in this paper. The efficiency validation of MFX solver has been performed first to evaluate the performance of this FSI software. Some tentative simulation cases closely related to ocean engineering has also been carried out. The main purpose of those simulations is to provide supplementary information on vortex wake for the model test and carry out advanced research on VIV before actual engineering applications.

2. Numerical Solution

2.1 FSI Strategy of Ansys

ANSYS MFX solver has been adopted to solve the FSI problems related to VIV of flexible risers/pipes in this paper. The well-designed ANSYS FSI solution strategy provides tightly integrated flow and structure physics. It offers designers and analysts a most flexible and advanced coupled structure－fluid physics analysis tool. In addition, the adoption of the implicit coupling iteration ensures that fluid and structure solution fields are consistent with each other at the end of each multi-field step. It leads to improved numerical solution stability (ANSYS, 2007).

2.2 Turbulence Model

Generally speaking, the discrepancy between experiments and numerical simulations partially attributes to the disability of turbulence model and the time-space resolution of the grids used in numerical simulation. Since the Reynolds numbers of all the simulation cases in this paper are relatively low, the LES model has been adopted for accurate prediction of vortex shedding.

3. Efficiency Validation of FSI Solution

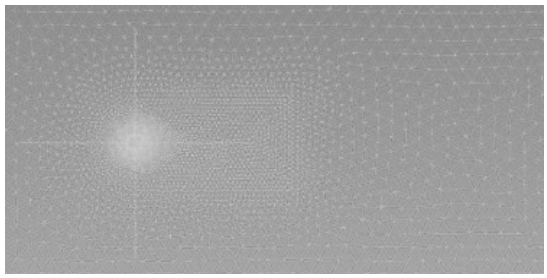

Fig. 1 Multi-blocked grid topology for flow field

Before applying the ANSYS MFX scheme to solve the VIV problem, two numerical simulations aiming at validating its efficiency for VIV problem have been accomplished. The first one relates to the published VIV experiment of a naked brass pipe under uniform and sheared currents, carried out by MARINETEK. The second one relates to the VIV experiment of long FRP pipe under sheared current which was carried out by KORDI.

3.1 Brass Pipe Under Uniform and Sheared Currents

In this VIV experiment, the riser model was made of a brass pipe with outer diameter of 20mm and wall thickness of 0.45mm. The effective length of the riser model was 9.63m. The tension imposed on the two ends was 817N. More information should refer to the description document of the VIV experiment (Lehn, 2003; Huang and Chen, 2009). Since the strain gauges and accelerometers were glued to the outside of the brass pipe surface, the riser diameter was locally increased at the instrumented sections (bumps). In the corresponding numerical simulation, the bumped riser was regarded as straight one with uniform section whose outer diameter is of 20mm and wall thickness of 0.45mm. In order to represent the original mass of instrumented section by compacted volume, the mass density of those special portions has been locally increased.

The grid system for VIV simulation of this pipe is designed to provide adequate flow resolution with a computable number of mesh nodes. The grid topology with refined mesh in the wake and around the riser and lower resolution in other fields was adopted, as shown in Fig. 1.

Two kinds of simulations related to the brass pipe system subject to uniform and sheared currents have been performed. It is worth noting that the sheared current speed has a linear profile with $U_{\min}$ (corresponding to the position '0' in Figs. 2~3) at bottom and $U_{\max}$

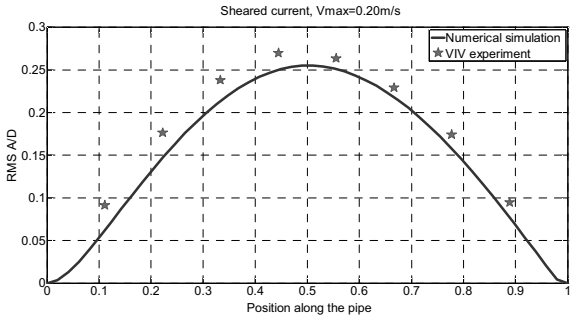

Fig. 2 RMS A/D pattern of cross-flow response along the brass riser span, in the case of sheared current Vmax=0.20m/s

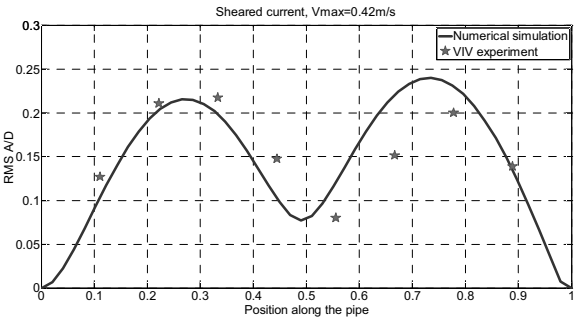

Fig. 3 RMS A/D pattern of cross-flow response along the brass riser span, in the case of sheared current Vmax=0.42m/s

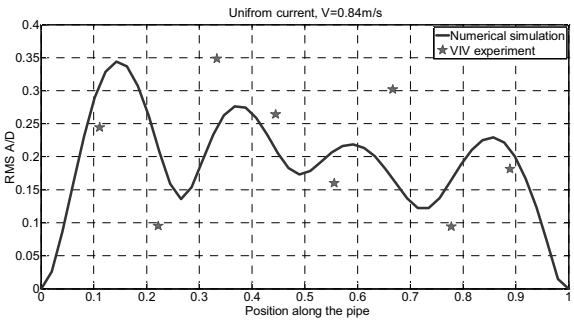

Fig. 4 RMS A/D pattern of cross-flow response along the brass riser span, in the case of uniform current V=0.84m/s

(corresponding to the position '1' in Figs. 2~3) at top, where U_{min}/U_{max} =0.14. Three cases, with U_{max} = 0.20m/s, 0.42 m/s, 0.56 m/s, were selected for the comparison between simulation and experiment in the case of sheared current. Another four cases with the uniform current velocity of 0.20 m/s, 0.42 m/s, 0.56 m/s, 0.84 m/s were presented to validate the efficiency of ANSYS multi-field software.

Three cases have been selected to demonstrate the efficiency validation result of numerical simulation. The RMS A/D (normalized instantaneous vibration amplitude) patterns of cross-flow response along the brass riser span in the case of sheared current of 0.20 m/s and 0.42 m/s and uniform current of V=0.56m/s were shown in Figs. 2~4, respectively. Generally speaking, the comparison result is encouraging. In the case of sheared current of 0.20m/s, shown in Fig. 2, the CFD simulation result agrees well with the observed data from model test case No. 1201. It was found that the disagreement became obvious when the sheared current rose to 0.42m/s. The magnitude and position estimation of the cross-flow response along the riser span deviated from the result of mode test case No. 1205 more or less, as shown in Fig. 3. No matter how the apparent waveform of the second mode consisted with that observed in VIV experiment. Larger disagreement has been found in the case of uniform current velocity equal to 0.84m/s, i.e. VIV experiment case No. 1108. However, the CFD simulation provided approximate RMS A/D pattern with corresponding experiment result, in spite of the position of modal component waveform is slightly different. In this case, the CFD method predicted that the 4th mode is the apparent dominant mode, while the experimental data indicated that both the 3rd and 4th modes have been excited simultaneously.

In a word, the estimation from numerical simulation shows comparatively good agreement with observed VIV experiment data in the engineering application point of view. The slight disagreements (in magnitude, position and dominant mode estimation) between simulated and experiment result results partially from the simplification process to replace instrumented sections with compacted uniform sections, and partially from the unpredictable effect of the rotation rig.

3.2 FRP RISER UNDER SHEARED CURRENT

The second VIV experiment used to evaluate the performance of the ANSYS MFX solver was carried out at KORDI in 2007. The riser length was of 16m and the outer diameter was of 39.7mm. The two ends of riser system have been 'pin to pin'supported with definite top tension imposed (Chen, Kim, 2008). Linearly sheared current was achieved by fixing one end of the riser and towing another by CPMC for a semicircular movement. The schematic view of the experimental setting was shown in Fig. 5.

Simulated results related to three cases with maximum inflow velocities V_{max} =0.5m/s, 1.0m/s, 1.2m/s (top tension: 100kN), were presented. The spectral comparison between

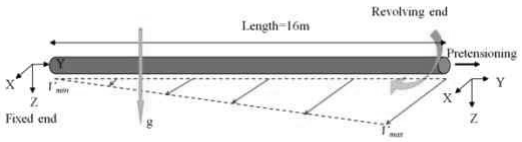

Fig. 5 The schematics of VIV experiment for long FRP riser model

measured (unit: $\mu\varepsilon$) and simulated (unit: A/D) results was shown in Figs. 6~8. In those figures, the blue-dashed line (namely, line 1) and red-solid line (namely, line 2) represent the power distribution of cross-flow and in-line riser vibration observed in model test. The green-circle-dotted line (namely, line 3) and magenta-square-solid line (namely, line 4) denote the power distribution of cross-flow and in-line riser vibration obtained by numerical simulation.

There is no evidence that the VIV along the riser occurs according to the Strouhal relation $S_t = f_v D/U$ or any other linear relationship. It is worth noting that the power spectra shown in Figs. 6~8 typically demonstrate the frequency-energy distribution of VIV at some position along the riser. From the frequency analysis of the three simulated cases, one could find that the dominant frequency of cross-flow vibration is mainly determined by towing speed of CPMC in model test. Similarly, the dominant frequency is determined by the maximum velocity of sheared flow in numerical simulation. The power spectra of numerical simulation and experiment is indeed a unimodal curve in the case of low sheared flow V=0.5m/s, shown in Fig. 6. When the sheared current velocity rises, some subordinate modes will be excited with considerable instantaneous amplitude (shown in Figs. 7 and 8). Nevertheless, the vibration energy of subordinate modes in cross-flow is still not comparable to the dominant one. From the spectral comparison shown in Figs. 6 and 7, one can promptly draw a conclusion that the apparent frequencies/modes observed in numerical simulation are consistent with those from VIV experiment. When the Reynolds number is relatively high, e.g., V=1.2m/s, as shown in Fig. 8, the disagreement between CFD estimation and VIV experiment becomes distinct. It mainly results from the fact that severe mesh distortion has been observed around the deformed riser. This would result in convergence difficulty in fluid field. Since the spring analogy is adopted in CFX solver to deal with mesh deforming problems, the intensity and amplitude of vibration response are limited for VIV simulation.

Overall, based on the spectral analysis result, one can

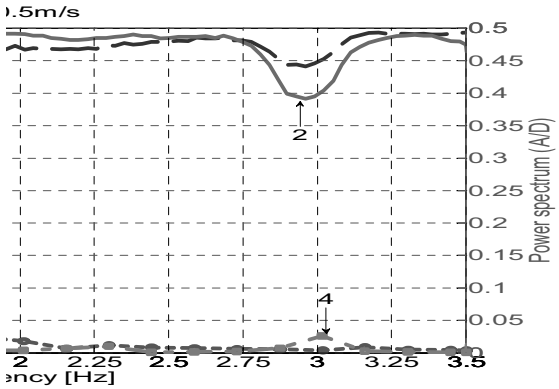

Fig. 6 Spectral comparison between measured and simulated results at V=0.5m/s

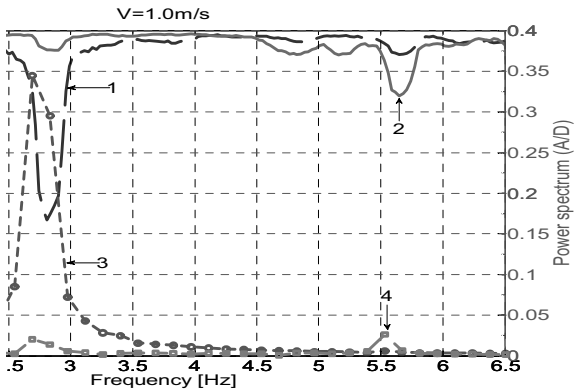

Fig. 7 Spectral comparison between measured and simulated results at V=1.0m/s

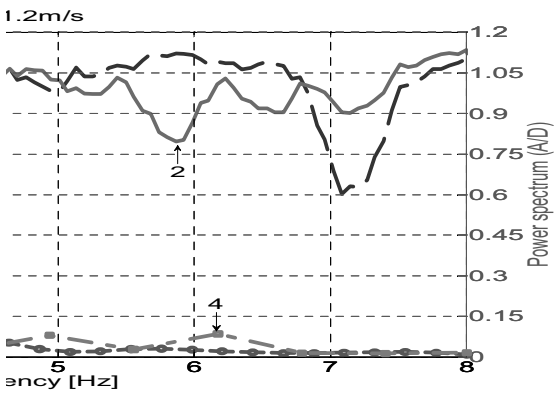

Fig. 8 Spectral comparison between measured and simulated results at V=1.2m/s

find that the numerical simulation shows good agreement with VIV experiment when the mesh distortion is not serious. In fact, the numerical simulations of VIV are usually characterized by large displacement and

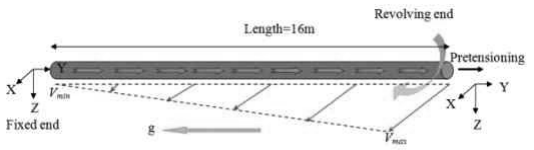

Fig. 9 The schematics of FRP long riser model with internal flow for the numerical simulation of VIV

considerable deformation. Considering the deficiency of the CFX solver in processing mesh deformation, the mesh control technique by means of User-Fortran and CEL would be adopted in the numerical simulations performed below. After the successful efficiency validation of the FSI solution approach, the following numerical simulations aiming at solving more complex VIV problem have be performed.

4. NUMERICAL APPLICATION TO VIV

4.1 EFFECT OF INTERNAL FLOW ON VIV

Although there are many works on the VIV study of flexible pipe/riser system which are subject to external current, the contribution of internal flow to the riser vibration mode has rarely been studied. In fact, the curvature of the flexible pipe/riser and the relative motion of axial flow to the time-dependent riser motion are the crucial factors to affect coupling mechanism between fluid and structure.

The following simulation case has been designed to make an investigation about the effect of internal flow on VIV. The riser model was similar with that described in the previous section of FRP long riser model with sheared current. Specially, the riser internal flow has been pumped from the fixed end to the revolving end. The direction of gravity acceleration has been changed into the reverse direction of internal flow. This modification tended to regard the riser system as a down scaled marine riser model with internal flow and external current considered at the same time. The schematic view of the setup for numerical simulation was demonstrated in Fig. 9.

A series of numerical simulations have been carried out with different combinations of external current velocities V_{max} (0.5 m/s and 1.0 m/s), internal flow velocities V_{int} (0.0 m/s, 0.5 m/s and 1.0 m/s), and top tensions T_{top} ($80kgf$ and $100kgf$).

Fig. 10-12 show the in-line (denoted as '1', '3', '5') and cross-flow (denoted as '2', '4', '6') vibration responses along the riser span at internal flow velocity of

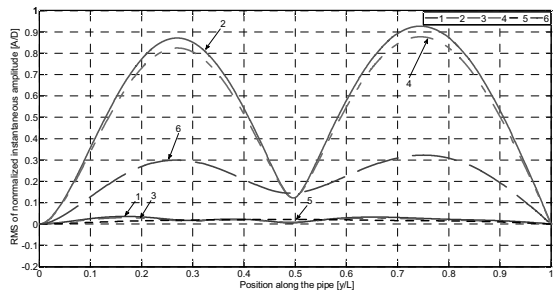

Fig. 10 The RMS of normalized instantaneous amplitude (statistic envelope) of in-line and cross-flow vibration at $V_{max} = 0.5m/s$ and top tension $T_{top} = 80kgf$

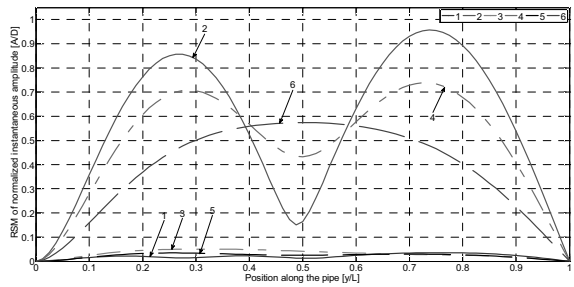

Fig. 11 The RMS of normalized instantaneous amplitude (statistic envelope) of in-line and cross-flow vibration at $V_{max} = 0.5m/s$ and top tension $T_{top} = 100kgf$

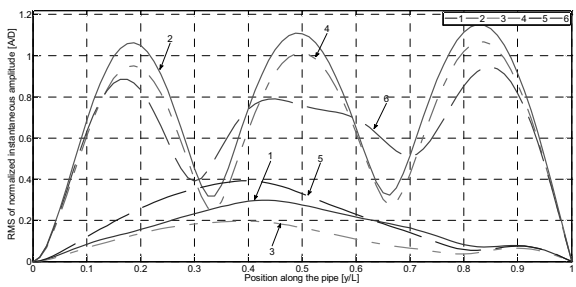

Fig. 12 The RMS of normalized instantaneous amplitude (statistic envelope) of in-line and cross-flow vibration at $V_{max} = 1.0m/s$ and $T_{top} = 100kgf$

0.0 m/s, 0.5 m/s, and 1.0 m/s, respectively. The conclusions from this simulation have been drawn as follows:

Firstly, it was found that magnitude of top tension plays an important role in determining the effect of riser internal flow. From the comparison between the two series shown in Fig. 10 ($V_{max} = 0.5m/s$, top tension $T_{top} = 80kgf$) and Fig. 11 ($V_{max} = 0.5m/s$, top tension $T_{top} = 100kgf$), one may conclude that the magnitude of top tension is a crucial factor to diminish or enhance the effect of riser

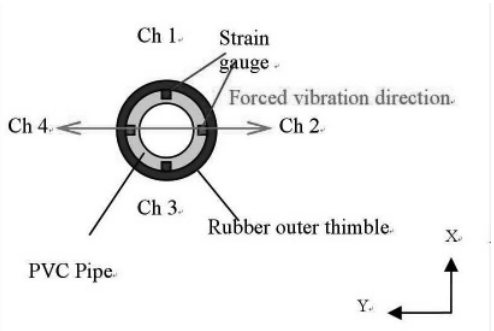

Fig. 13 The configuration of the PVC pipe used in model test

internal flow on VIV. As it was shown in Fig. 11, the effect of riser internal flow may be enlarged in the case of high top tension, while its effect may be weakened when the top tension is at small value of 80kgf.

Secondly, the existence of internal flow is an important factor to determine the vibration amplitude of the riser system. It becomes obvious when the top tension is relatively high and the velocity ratio of external current against internal flow is relatively low. This conclusion is clearly demonstrated by the comparison between Figs. 11 and 12, in which the same top tension and different external current velocity were given. When internal flow speed rises, the amplitude of cross-flow vibration decreases distinctly in both cases. As a rule, the larger the velocity ratio of internal flow against external current is, the less the vibration amplitude along the riser span would be.

Finally, the existence of internal flow contributes much to determine the vibration mode of the flexible riser model, or even changes the vibration mode eventually. This conclusion has been well demonstrated by Fig. 11. It was found that the second vibration mode of cross-flow, denoted as the '4' curve, was weakened with the increase of internal flow speed, in the case series of $V_{max} = 0.5m/s$ and $T_{top} = 100kgf$. When the magnitude of internal flow speed rose to V_{int} = 1.0m/s, the vibration mode switched from the second natural vibration mode to the first vibration mode entirely. Similarly, the third vibration mode was weakened with the increase of internal flow speed, in the case series of $V_{max} = 1.0m/s$ and $T_{top} = 100kgf$, as shown in Fig. 12. Contrasting to the case of $V_{max} = 0.5m/s$ and $T_{top} = 100kgf$, the larger magnitude of internal flow leads to the appearance of multi-modal phenomenon (3th and 4th coexistence). It is obvious that higher order of vibration mode would be easily excited in the case that the internal flow and external current are high simultaneously. The function of external current in the coupling system is to determine the vibration mode of riser model, while the effect of internal flow is to alter the equilibrium VIV state.

In a word, the comparison between simulation cases with and without internal flow shows that the existence of internal flow plays an important role in changing the dominant frequency, as well as the instantaneous vibration amplitude. Its effect would be amplified when the magnitude of top tension is high and the velocity ratio of external current against internal flow is relatively low.

4.2 PVC Pipe Subject to Forced Motion

The model test upon which this simulation case is based has been performed at KORDI (Choi and Hong, 2000). In the model test, the forced sinusoidal oscillation was imposed on a 3.4 m long PVC pipe. The pipe external diameter is of 53.8 mm, coated by rubber. The upper pipe end was forced to move in a sinusoidal trajectory with definite amplitude. Another end was drawn by an object weight 1kg, free to vibrate in 6-DOF directions. The frequency of forced sinusoidal oscillation varied from 0.2 Hz to 2 Hz.

The objective of this simulation was to provide some supplementary information on vortex wake shedding to VIV experiment and give interpretation to the unique oscillation phenomena of pipe. The schematic view of the forced oscillation system was shown in Fig. 13.

In general, the velocity vectors vary with the pipe deformation. However, the relative position of velocity is o-surface to pipe displacement was comparatively steady, even in the case of severe deformation happening. In other words, the configuration of velocity is o-surface which is induced by forced vibration and VIV is indeed a measurement of vibration intensity, just as instantaneous normalized amplitude does. Four cases related to the forced frequency of 0.61Hz, 1,06Hz, 1.43Hz, 1.60Hz (denoted as cases 2, 3, 5, and 6, respectively, in Fig. 14) have been selected to show the configuration variance of velocity is o-surface.

The blue opaque envelope represents the velocity is o-surface of V=0.02m/s, and green semi-transparent envelope denotes the velocity is o-surface of V=0.01m/s. The second vibration could be easily observed among those four figures with dumbbell-like wake pattern. The fact that the periphery of is o-surfaces at pipe ends were larger than that at other sections is considered as the 'end effect' (Michael, 1994). In case of small frequency with small normalized instantaneous amplitude, e.g. cases 2 and

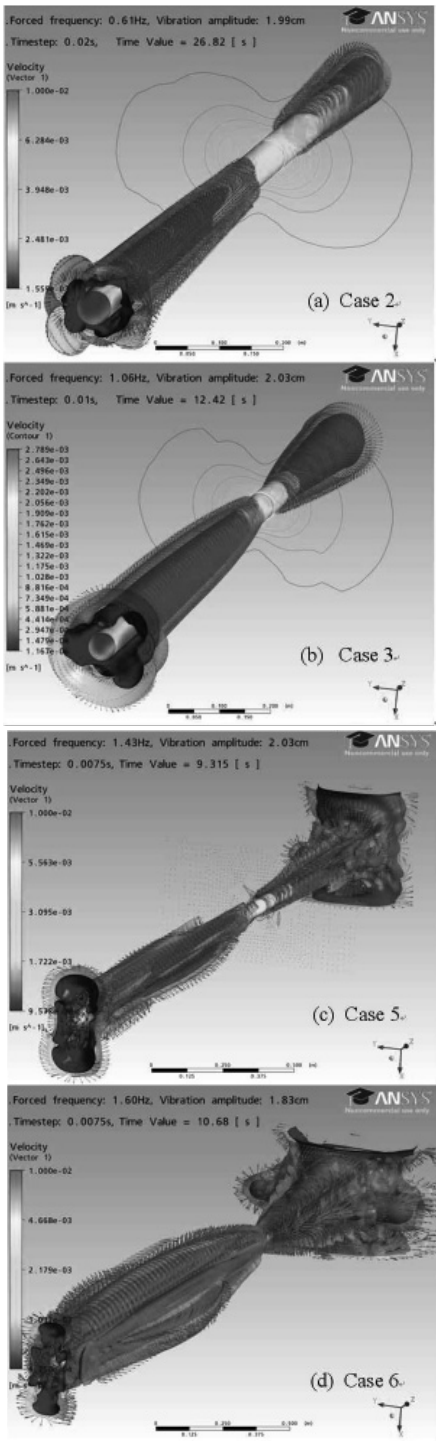

Fig. 14 The velocity iso-surface visualization around the oscillating PVC pipe at different frequencies

3, the two configuration of velocity is o-surface are composed of a couple of conical shapes.

When the frequency rose, the velocity is o-surface pattern changed a lot. In cases5 and 6, the conical velocity is o-surface turns into complicated envelope. The magnitude variation of Y-direction (in-plane) velocity vector along the upper 2/3 pipe length is much larger than that of X-velocity (out-of-plane) at the forced oscillation end. It results from the fact that the intensity of in-plane oscillation had been enhanced due to high oscillation frequency. The emergence of 'end effect' parti all

results from the existence of pipe internal flow induced by the coupled effect of the in-plan forced oscillation and out-of-plan vortex-induced vibration frequency. Therefore, the 'end effect' at pipe free end (outflow of vibration-induced internal flow) was extremely magnified when oscillation frequency rose, shown in subplots (c) and (d) of Fig. 14.

Although the deformation of out-of-place has several orders of magnitude less than that of in-place, the velocity magnitude in the two directions (on the same section) is comparable. The Y-axis velocity component mainly results from the in-place large displacement and deformation induced by forced oscillation. The X-axis velocity component is mainly due to the vortex-induced vibration of out-of- plane. Since the magnitude of velocity vector induced by VIV has the same order of magnitude with the former, it should not be neglected. Hereon, we can draw a conclusion that the out-of-plane vortex-induced vibration with relatively small amplitude contributes to vortex wake and pipe structural deformation as much as the forced oscillation with large amplitude.

4.3 Flexible Multi-Assembled Pipe Systems

The main purpose of this section is to study the VIV phenomena of multi-assembled risers which are commonly used in offshore oil production. Dual and quad-pipe systems have been taken into account in the following numerical simulation with focus on the interaction between front and rear pipes. The riser model was made of PVC pipes with outer diameter of 50mm and wall thickness of 2.5mm. The total depth of the tank was of 3m. Water current was given in the lower part of tank with the water height of 2.5m, while the upper part of tank was filled with stationary air. Specially, the riser internal flow has been pumped from the lower end to the upper end of the rear pipe. The basic configuration of the numerical simulation and detailed boundary conditions were shown in Fig. 15.

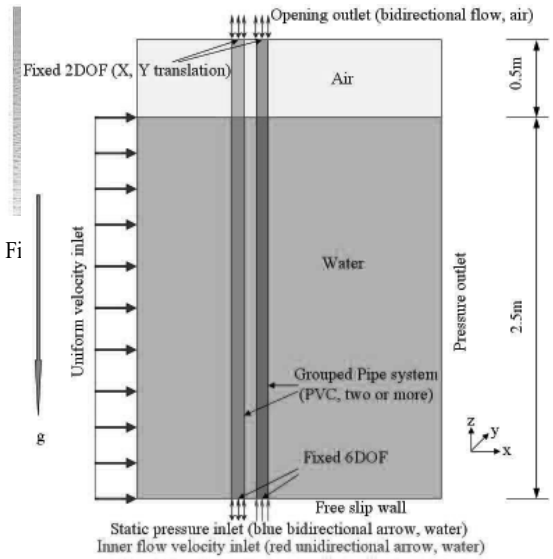

Fig. 15 The configuration of the multi-pipe system and the boundary conditions in numerical simulation

The vortex modes were kept steady when physical parameters, such as d (distance between pipes), V_r (reduced velocity), Re (Reynolds number) were fixed. The 2S shedding mode (single vortex both sides) is prevailing in most simulation cases. Since the length of flexible pipe is not long enough to permit considerable vibration amplitude, the 2P shedding mode (a pair of vortices both sides) has not been observed in those cases.

In the case of $d = 3D$ (at different current velocities), only 2S vortex mode has been observed. In the case of the two pipes in tandem being closer, e.g. 2D in this paper, the destruction, retardation and reconstruction of vortices affected the vortex formation in the wake distinctly. Those effects enlarged the magnitude of velocity component which was towards the tail of front pipe, leading to the decrease of drag coefficient. In the dual-pipe system, the magnitude decrease of drag coefficient was considerably large, comparing to the influence on cross-flow vibration. In most cases of $d = 2D$, neither the amplitude nor the oscillation frequency was constant, for the shear layer and vortex structure have never been sufficiently established. The P+S vortex shedding pattern(a pair of vortices and single vortex each side) has been observed in the vortex wake around the pipe mid-span in the case of $d = 2D$, $V_{ext} = 0.6m/s$. It resulted from the fact that the coupling becomes distinct when the pipes in tandem are closer and inflow current

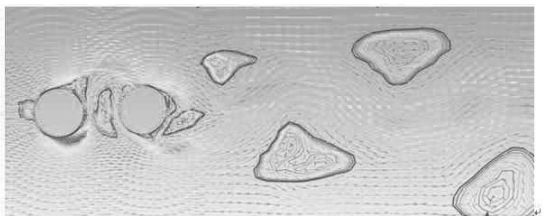

Fig. 16 Vortex shedding pattern in the case of $d = 2D$, $V_{ext} = 0.4m/s$, at position $Z = 1.8m$

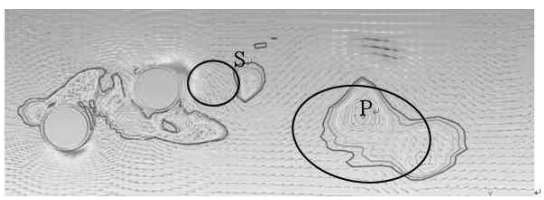

Fig. 17 Vortex shedding pattern in the case of $d = 2D$, $V_{ext} = 0.6m/s$, at position $Z = 1.8m$ (P+S type vortex model appears with enlarged amplitude)

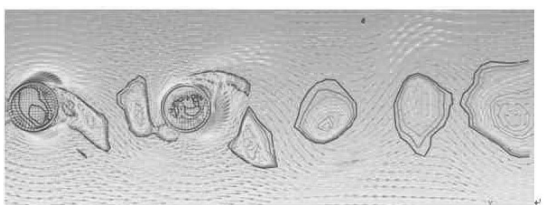

Fig. 18 Vortex shedding pattern in the case of $d = 3D$, $V_{ext} = 0.4m/s$, at position $Z = 1.8m$

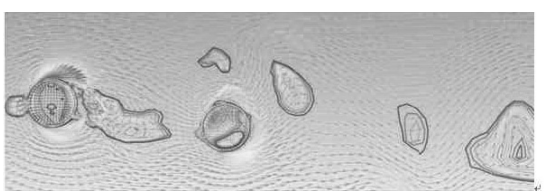

Fig. 19 Vortex shedding pattern in the case of $d = 3D$, $V_{ext} = 0.6m/s$, at position $Z = 1.8m$

velocity is larger. In this case, the existence of rear pipe played an important role to reconstruct the vortex conformation behind the front pipe. It resulted in considerable amplitude in cross-flow and velocity fluctuation from cycle to cycle in the dual-pipe system.

Contrasting to those conclusions drawn from long FRP riser model, one can find that the effect of internal flow on VIV of rear pipe is restricted due to the small L/D aspect ratio of the pipes adopted in the present study. It is worth noting that the existence of internal flow slightly enhanced the cross-flow VIV and dominant frequency in

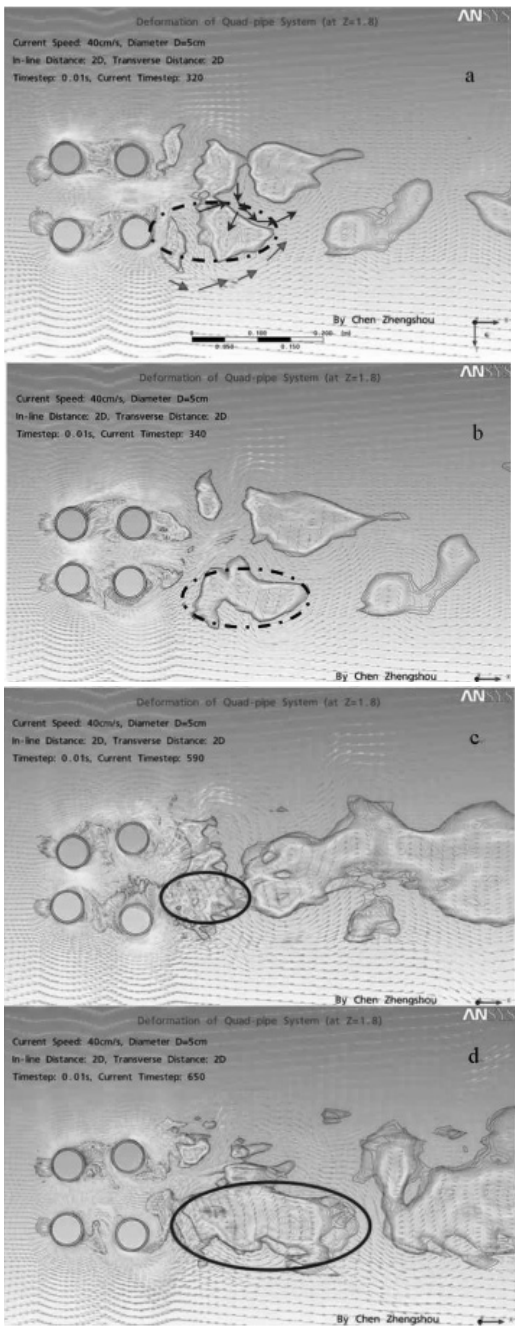

Fig. 20 Vortex visualization for the case of quad-pipe system confined by 2D in-line and 2D cross-flow with $V_{ext} = 0.4m/s$, at $Z = 1.8m$

the case of $V_{ext} = V_{in} = 0.4m/s$. However, the external current velocity and the distance between two pipes were still the critical factors to determine the vibration state of

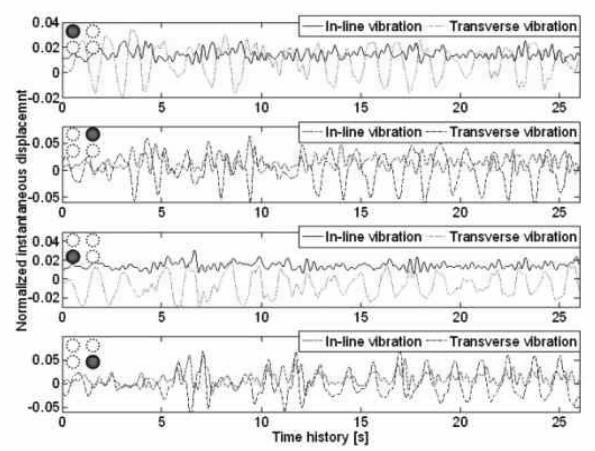

Fig. 21

the dual-pipe model.

Furthermore, the VIV simulation for the quad-pipe arrangement (center-to-center distance of 2D in-line and 2D cross-flow) has been performed, at current velocity of V_{ext} =0.2m/s, 0.4m/s. The vortex shedding pattern and normalized instantaneous displacement (to D) for this quad-pipe system at external current velocity of V_{ext} =0.40m/s and 0.20m/s were shown in Figs. 20 and 21(the position of the demonstrating pipe was marked by red color), respectively.

In the case of V_{ext} =0.40m/s, it is quite certain that the vortex shedding patterns shown in Fig. 20, were more complex than those observed in dual-pipe system. Among those unique vortex visualizations, there were some fields where the vortex region was enlarged, shown in sub plots (c) and (d) of Fig. 20. It resulted from the fact that the rolling directions of the two S-type vortices coming from two adjacent rear pipes were co-rotating. However, there were some regions that the vortex formation was shrunk or even disappeared when vortex directions of adjacent vortices were contra-rotating, shown in sub plots (a) and (b) in Fig. 20.

In the case of V_{ext} =0.20m/s, shown in Fig. 21, both in-line and cross-flow vortex-induced vibrations were similar with those observed in single-pipe system, for the reduced velocity was not large enough to excite high frequency vortex shedding and structural vibration. The instantaneous oscillation amplitude of in-line vibration was an order of magnitude lower than that observed in cross-flow vibration. Although the backflow had been enhanced due to the existence of downstream pipe, it was found that it had little influence on the drag coefficient of

front pipes.

Similar with that observed in the case of dual-pipe system, the vortex shedding formation was controlled by the existence of the rear pipes at low external flow velocity. However, the periodic vibration state would be destroyed more quickly than dual-pipe system when the reduced velocity became higher, e.g. V_{ext} =0.40m/s in this paper. In addition, due to the mutual restriction from adjacent pipes in cross-flow and in-line simultaneously, both the RMS values of in-line and cross-flow VIVs were larger than those observed in dual-pipe system.

5. CONCLUSIONS REMARKS

A series of VIV-related studies with the focus on flexible risers subject to various engineering conditions have been performed in this paper. The main conclusions have been drawn as follows:

1) Two numerical simulation cases based on VIV experiment have been carried out to validate the calculation efficiency of ANSYS MFX solver designed for FSI solution. It has been confirmed that it is able to give an acceptable estimation to VIV simulation related to flexible pipe systems even at considerable Reynolds number, if the occurrence of severe mesh distortion could be well solved.

2) Important findings from the numerical simulation contribute much to a reasonable interpretation of the coupling mechanism between VIV and vortex wake in the form of providing supplementary information of vortex visualization and structural deformation simultaneously.

3) Some tentative cases accomplished by numerical simulation reveal some new findings related to complex pipe systems. The result from the VIV simulation involving internal flow shows that the effect of internal flow is sensitive not only to external current velocity but to top tension. The result from forced oscillation simulation shows the VIV contributes to vortex wake and pipe structural deformation as much as the forced oscillation with large normalized amplitude.

ACKNOWLEDGEMENT

This work was financially supported by the Korea Research Foundation Grant funded by the Korean Government (MOEHRD, Basic Research Promotion Fund) (KRF-2008-D00556) and Mokpo National University RIC for Midsize Shipbuilding.

REFERENCES

[1] 2007, ANSYS, "ANSYS CFX-Solver Modeling Guide (V11 SP1)", ANSYS Co.

[2] 2008, Chen, Z.S. and Kim, W.J., "Numerical simulation of a large-scale riser with vortex-induced vibration," *Proceedings of the Eighth ISOPE Pacific/Asia Offshore Mechanics Symposium*, Bangkok, Thailand, November 2008.

[3] 2000, Choi, Y.L. and Hong, S., "Study about structural deformation estimation about flexible pipe in the engineering basin model test," *Korea Ocean Research & Development Institute (KORDI)*, *Research report*.

[4] 2006, Holmes, S. and Owen, H., "Simulation of Riser VIV Using Fully Three Dimensional CFD Simulations," *OMAE*, Hamburg, Germany.

[5] 2009, Huang, K. and Chen, H.C., "Vertical Riser VIV Simulation in Sheared Current," *ISOPE*, Osaka, Japan.

[6] 2003, Lehn, E., "VIV suppression tests on high L/D flexible cylinders (main report)," *Exxon Mobil upstream research company*.

[7] 2006, Menter, F. and Sharkey, P., "Overview of Fluid-structure coupling in ANSYS-CFX," 2*5th International Conference on Offshore Mechanics and Arctic Engineering*, Hamburg, Germany.

[8] 1994, Michael, S.P., "Vortex induced vibration parameters: critical review," *OMAE Offshore Technology*, U.S.A.

[9] 2004, Yamamotoa, C.T. and Meneghinib, J.R., "Numerical simulations of vortex-induced vibration on flexible cylinders," *Journal of Fluids and Structures*, Vol.19, pp.467-489.